RESEARCH ARTICLE

Advancements in Amorphous Solid Dispersions to Improve Bioavailability

Prediction and Construction of Drug-Polymer Binary System Thermodynamic Phase Diagram in Amorphous Solid Dispersions (ASDs)

Zhiqing Hu[1] · Pengchong Xu[1] · Eman A. Ashour[1] · Michael A. Repka[1,2]

Abstract

Amorphous solid dispersion (ASD) has been well known as a potential strategy to improve the bioavailability and dissolution performance of poorly water-soluble drugs. The primary concern of this approach is the long-term stability of the amorphous drug in the solid dispersion. Accurate prediction and detection of the solubility and miscibility of drug in polymeric binary system will be a milestone to the development of ASDs. In this investigation, a method based on Flory–Huggins (F–H) theory was proposed to predict and calculate the solubility and miscibility of the drug in polymeric matrix and construct the phase diagram to identify the relevance between drug loading and temperature for ASDs development. Indomethacin (Indo) was chosen as the model drug, and polyvinyl pyrrolidone vinyl acetate (Kollidon® VA 64) was used as a polymeric carrier for the ASD systems. Physical mixtures were prepared with different drug loadings (10 to 90%) and analyzed by differential scanning calorimetry (DSC). The interaction parameter χ was calculated for physical mixtures by the melting point depression and solubility parameter contribution methods. The phase diagram was constructed to investigate the impact of other parameters like drug loading, processing temperature, and Gibbs free energy of mixing (ΔG_{mix}). For further validation, formulations were developed using HME to verify the accuracy of the phase diagram and to guide in the hot-melt extrusion (HME) process design space and optimization.

KEY WORDS flory–huggins theory · amorphous solid dispersions · melting point depression · hot-melt extrusion · phase diagram · miscibility · formulation

INTRODUCTION

In recent decades, developing amorphous solid dispersions has become an attractive strategy for improving compound solubility, dissolution rate, and oral bioavailability (1–4). The drug aqueous solubility can be significantly increased once combined into a dispersed system compared to its crystalline form. However, the Gibbs free energy is higher for the amorphous state than the crystalline state, so the amorphous drugs usually have long-term stability concerns and challenges because of the quick recrystallization tendency during processing and storage (5–7). There are many ways to improve the stability of the amorphous drugs, such as selecting proper polymeric carriers and proper drug loading for the formulation, allowing the drug to disperse into the polymeric matrix, and forming a stable amorphous solid dispersion (8). Therefore, there is an urgency to develop a method to select the suitable polymer and the optimum drug loading that could help the stabilization of the ASD formulation (7).

Even though ASD can help improve the solubility of poorly water-soluble drugs, the selection of polymer type is essential to stabilize the high-energy nature of ASD. The miscibility of a drug and a polymer system is essential since the specific interaction between the drug and polymer is critical for the stability of the ASD system. Another critical factor that needs to be considered when producing ASD

✉ Michael A. Repka
  marepka@olemiss.edu

1 Department of Pharmaceutics and Drug Delivery, School of Pharmacy, The University of Mississippi, University, MS 38677, USA

2 Pii Center for Pharmaceutical Technology, University of Mississippi, University, MS 38677, USA

formulation is the amount of drug loading integrated into the polymeric matrix. High drug loading can cause instability of the dispersion system and further recrystallization, which leads to solubility reduction (9).

Developing a one-phase drug-polymer binary system requires the two components (drug and polymer) to be thermodynamically miscible; also, the process parameters need to be optimized during this production (10). The most common methods to prepare ASDs are hot-melt extrusion (heat-based) and spray drying (solvent-based) in the pharmaceutical industry (3). Furthermore, since the preparation of ASDs may occur at non-ambient temperatures or in the presence of organic solvents, disturbance of the system during operation can guide a dynamic system that re-equilibrates after processing (11). A more relevant and logical approach would be beneficial to comprehend the miscibility degree of a drug in a polymeric matrix as a function of temperature and how this might be connected to the molecular structure and physical characteristics of the drug-polymer combination. (12, 13). It would be contributory in identifying better drug-polymer compositions that form strong interactions between them by implementing simple experimental methods. The construction of a phase diagram could guide the selection of ideal drug loading and optimize processing conditions to maximize the stability of the ASD formulation (11, 14, 15).

HME has been extensively explored as one of the development strategies for preparing ASDs, which improves the solubility and bioavailability of poorly water-soluble drugs (BCS class II and class IV). HME provides several advantages compared to the solvent-based method for thermally stable materials, including an eco-friendly, solvent-free, low-cost, continuous, and accessible processing method (2). HME is an application that combines mixing, melting, softening, and conveying simultaneously. The optimization of the HME process in the pharmaceutical area has been investigated by formulation development, process parameters, and other factors (2, 7).

In the present study, the melting point depression method was evaluated using DSC measurements based on the Flory–Huggins (F–H) theory, in which the F–H interaction parameter (χ) could be determined from the mixture of different combinations of drug and polymer system (12, 16, 17). Recent studies reported that χ is not only drug loading-dependent but also temperature-dependent (18–20). Gibbs free energy of mixing (ΔG_{mix}) was not favorable when χ was positive, indicating immiscibility between the drug-polymer system. Conversely, when χ had a negative or slightly positive value, the ΔG_{mix} was negative, implying that the drug and polymer system was miscible. This research will allow for a better understanding of F–H interaction theory for drug-polymer miscibility suggestions during processing and the choice and loading limit of the drug and polymeric carrier. This research aimed to build and construct

the phase diagrams that can provide thermodynamics information through different processing conditions, including the relationship between drug loading, temperature, and phase transitions and separation. This binary phase diagram allows predicting the solubility and miscibility of different drug-polymer systems (16, 18). Building phase diagrams that significantly correlate with experimental measurements and product states would benefit formulation development studies (13, 14).

The acquired data will guide the HME design space map for extruded ASDs preparation. Additionally, the study aimed at providing a logical and reasonable discussion on how this phase diagram can be used to evaluate the appropriate drug for the ASD system (21, 22) and also validated the prediction from the phase diagram by executing the HME based on the suggested information and utilized phase diagram validation to evaluate the stability analysis. The model drug selected in this investigation was indomethacin (Indo), a BCS class II (low solubility, high permeability) compound, and Kollidon® VA 64 was chosen as a polymeric carrier for ASDs.

MATERIALS AND METHODS

Materials

Indomethacin was purchased from TCI (Tokyo Chemical Industry Co., Ltd., Tokyo, Japan); Kollidon® VA 64 grade was gifted from BASF (Florham Park, NJ, USA). The chemical structure of the indomethacin and Kollidon® VA 64 are shown in Fig. 1.

Sample Preparation

Indomethacin and Kollidon® VA 64 were stored in a vacuum drying oven at 40 °C, 200 mbar at least 2 days before further investigation. Then, different drug loadings 10, 20, 30, 40, 50, 60, 70, 80, and 90% (w/w) were mixed with Kollidon® VA 64 using MaxiBlend™ blender (GlobePharma Inc., New Brunswick, NJ, USA) at 30 RPM for 10 min to ensure an even distribution of chemicals (total weight 10.0 g per batch).

Drug and Polymer Thermal Stability Analysis

DSC and TGA tests were performed to verify the drug and polymer thermal stability and provide information about their physical state and thermal behavior for future analysis. For the DSC test, TA DSC 25 (TA Instruments, New Castle, DE, USA) was used in this research. Around 5 mg of each drug/polymer physical mixture with different drug loading was packed into a T_{zero} hermetic aluminum pan (TA

Fig. 1 Chemical structure of **a** indomethacin and **b** Kollidon® VA 64
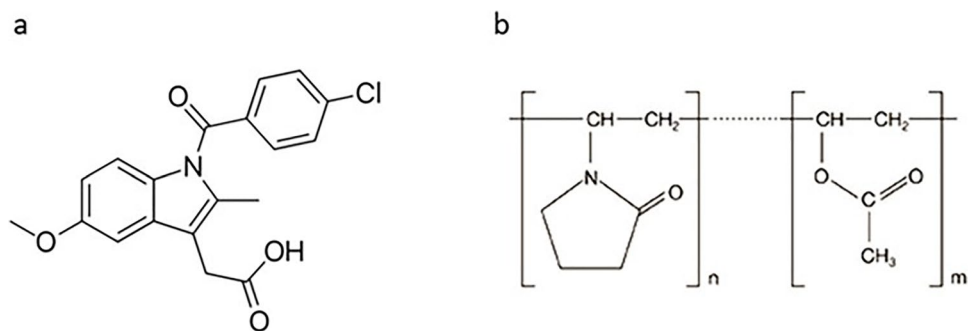
Instruments, Waters, LLC, USA) with a lid. A pinhole was made into the lid to allow the moisture to escape. DSC was conducted at a heating rate of 10 °C/min from 0 to 200 °C. For the TGA test, approximately 5–10 mg drug/polymer were placed in a platinum pan with a heating rate of 10 °C/min from 25 to 200 °C to check the sample weight loss with the heating flow. Nitrogen was used as the purge gas for both tests.

Glass Forming Abilities (GFA)

GFA is a classification system based on drugs recrystallization behavior during DSC heat-cool-heat cycles. GFA class 1 defines drugs that will recrystallize at a cooling section with a cooling rate of 20 °C/min; GFA class 2 includes drugs that will recrystallize at the 2nd heating ramp with the heating rate of 10 °C/min, while class 3 drugs will not recrystallize either at a 20 °C/min cooling rate or at the 10 °C/min 2nd heating ramp [23, 24]. This GFA classification system allows for more understanding about the glass-forming behavior of drugs and guides to make better decisions of the suitable drug for ASD development with long-term stability.

Melting Point Depression (MPD) Method

Modulated DSC (MDSC) was used for the MPD method, where nitrogen was used as the purge gas. The modulation amplitude applied over the entire method was 1 °C every 60 s for the mixtures of Indo and Kollidon® VA 64. Around 5 mg sample was packed into a T_{zero} pan (TA Instruments, Waters, LLC, USA) with a lid. A pinhole was made in the lid to allow the moisture to escape. An initial drying step with a heating rate of 10 °C/min to 80 °C was used to remove residual moisture from the system before the heat-cool-heat cycle since the moisture could interfere with the DSC heat flow measurements. DSC was set up after the initial heat cycle to equilibrate at 0 °C for 5 min. Melting depression experiments were conducted at a heating rate of 2 °C/min from 0 to 200 °C and allowed to re-equilibrate for 5 min to make sure the compound and

polymer are totally melted, followed by a jump cooling step to 0 °C and then isothermal step for 5 min again. The DSC pans were then reheated at 2 °C/min to 200 °C. The start point of the endothermic melting peak (T_m onset) was computed by the Trios software (TA Instruments, Waters, LLC, USA) and used for the calculation in this research.

This heat-cool-heat cycle was performed as mentioned above to identify the T_m and T_g of drug-polymer solid dispersion. T_m was estimated from the 1st heating ramp and the T_g from the 2nd heating ramp. This T_g value represented the neat T_g of freshly prepared ASDs when only a single T_g appeared in this section.

Theoretical Considerations

From the Gordon-Taylor (G-T) equations (Eqs. 1, and 2), if the drug-polymer are miscible, there should only be a single T_g for this binary system, and this T_g value can be predicted by the equation below:

$$T_{gmix} = \frac{(w_1 T_{g1} + K w_2 T_{g2})}{(w_1 + K w_2)} \tag{1}$$

$$K = \rho_1 T_{g1} / \rho_2 T_{g2} \tag{2}$$

where, T_{gmix}, T_{g1}, and T_{g2} are the glass transition temperature of ASDs, pure drug, and pure polymer, respectively; w_1 and w_2 are the drug and polymer weight fraction, respectively; ρ_1 and ρ_2 are the drug and polymer density, respectively; and K is the adjustable fitting parameter calculated by drug and polymer densities and T_g.

According to F–H theory, the change in Gibbs free energy of mixing for drug-polymer binary solid dispersions can be described as below (Eq. 3):

$$\Delta G_{mix} = \Delta H_{mix} - T * \Delta S_{mix} \tag{3}$$

where ΔG_{mix}, ΔH_{mix}, and ΔS_{mix} are the change in Gibbs free energy of mixing, enthalpy, and entropy and T represents temperature in kelvin.

Then, Gibbs free energy of mixing can be calculated by F − H drug-polymer interaction parameter, χ as shown in Eq. 4.

$$\frac{\Delta G_{mix}}{RT} = \varphi\ln\varphi + \frac{(1-\varphi)}{m}\ln(1-\varphi) + \varphi(1-\varphi)\chi \tag{4}$$

where φ and 1-φ are the volume fraction of drug and polymer, respectively. χ is the F–H interaction parameter, R is the molar gas constant, T is the temperature in kelvin, m is the ratio of the volume of a polymer chain to drug molecular volume, and it can be calculated by Eq. 5:

$$m = \frac{\frac{M_{W2}}{\rho_2}}{\frac{M_{w1}}{\rho_1}} = \frac{M_{W2} * \rho_1}{M_{w1} * \rho_2} \tag{5}$$

M_{w1} and M_{w2} are the molecular weights of drug and polymer, respectively, and ρ_1 and ρ_2 are the densities of drug and polymer. ΔG_{mix} can be calculated by Eq. 4 at a specified temperature and the corresponding interaction parameter. MPD DSC data from the different compositions can be used to predict the interaction parameter using the following equation (Eq. 6):

$$\frac{1}{T_m} - \frac{1}{T_{mo}} = -\frac{R}{\Delta H}\left[ln\varphi + \left(1 - \frac{1}{m}\right)(1-\varphi) + \chi(1-\varphi)^2\right] \tag{6}$$

where T_m and T_{m0} are the melting points of the drug crystal in the drug/polymer physical mixture and the pure drug, respectively, and ΔH is the heat of fusion of the drug. It should be noted that the interaction parameter χ is not constant but temperature- and composition-dependent. To develop a phase diagram to accommodate temperature variation, it defines the temperature dependence of the F–H interaction parameter χ as shown in Eq. 7 below:

$$\chi \cong A + \frac{B}{T} \tag{7}$$

where A is the value of the temperature-independent term for entropic contribution and B is the value of the temperature-dependent term for enthalpy contribution; the relationship has been simplified as this equation and has proven to be sufficient in many drug-polymer systems exhibiting an upper critical solution temperature (UCST). The first-order relationship between χ and $1/T$ has been used to extrapolate the value of χ for drug-polymer binary systems outside experimental temperatures. In this study, we have employed this equation that relates χ to temperature and used this to identify F–H constants A and B. Suppose the relationship between χ and T within a given temperature range can be determined for specific drug-polymer binary systems. In that case, ΔG_{mix} *versus* composition and temperature may be constructed by combining Eqs. 4, 6, and 7. Furthermore,

the maximum drug-polymer miscibility boundary (spinodal curve) may be calculated by determining the second derivative of the free energy (Eq. 7) and setting equal to zero as shown in Eq. 8 below:

$$\frac{1}{\varphi_{drug}} + \frac{1}{m * \varphi_{poly}} - 2\chi_{drug-poly} = 0 \tag{8}$$

where the interaction parameter χ can be substituted from Eq. 7, thereby, the maximum drug-polymer miscibility curve may be obtained.

Prediction of Solubility/Miscibility Using Drug and Polymer Solubility Parameters

In this research, the Van Krevelen group contribution method (25) has been used to calculate the solubility parameter δ_t of indomethacin and the polymer, which may be expressed as Eq. 9:

$$\delta_t = \sqrt{\delta_d{}^2 + \delta_p{}^2 + \delta_h{}^2} \tag{9}$$

where δ_d and δ_p and δ_h are the components of disperse forces, polar group forces, and hydrogen bond energy, respectively; these forces can be calculated as follows in Eqs. 10, 11, and 12.

$$\delta_d = \frac{\sum F_{di}}{V} \tag{10}$$

$$\delta_p = \frac{\sqrt{\sum F_{pi}{}^2}}{V} \tag{11}$$

$$\delta_h = \sqrt{\frac{\sum E_{hi}}{V}} \tag{12}$$

where F_{di} is the group contribution to the disperse forces, E_{hi} is the group contribution to hydrogen bonding energy, and F_{pi} is the plane symmetry factor of polar groups. The values of F_{di}, F_{pi}, and E_{hi} of each group at 25 °C used in this work were chosen from Van Krevelen's solubility parameters (25).

Therefore, the drug-polymer interaction parameter χ may be calculated as follows (25).

$$\chi = \frac{V_0}{RT}(\delta_{drug} - \delta_{polymer})^2 \tag{13}$$

where V_0 is the group contributions to the molar volume, the volume of the lattice site, and the molar volumes of a single polymer unit calculated from the group contributions that were used for the drug-polymer system. As shown in Eq. 13, χ refers to the square of the difference in solubility

parameters calculated from the values of group contributions at 25 °C. The drug-polymer interaction parameters for the Indo-based systems as calculated from solubility parameters (group contribution method) compared with the results were obtained from the melting point depression method.

Application of Phase Diagram for HME Process Map

The composition temperature phase diagram based on the F–H theory introduced before can also be applied to the HME to understand further and optimize the formulation performance and process development. The process design space that needs to be constructed is bounded by the drug-polymer solubility curve and the drug-polymer thermal degradation range (26). Polymer T_g and the minimum processing temperature (T_{min}) were also introduced to the design map to provide the viscosity requirements—with the lower drug loading—for the process; it was reported that most polymers need at least 10 °C above the polymer T_g (usually 10–15 °C above T_g) to ensure the drug will be molten (27, 28).

Preparation of Amorphous Solid Dispersions Through Hot Melt Extrusion: Validation of the Phase Diagram

ASDs were prepared by HME in order to validate the impacts of processing parameters on extruded filaments' characteristics. The HME processing conditions are clearly suggested previously from the temperature-composition phase diagram, which implied the temperature should be above T_{min} (around 120 °C) and under T_{deg} (around 200 °C). Amorphous solid dispersions of 20% and 40% drug loading of indomethacin in Kollidon® VA 64 were selected for investigation. The physical mixtures (PM) of Indo and Kollidon® VA 64 (total batch of 100 g) were prepared at the weight ratios and thoroughly blended for 30 min at 30 RPM by MaxiBlend™ blender (GlobePharma Inc., New Brunswick, NJ, USA).

The ASDs were prepared by a Thermo Scientific™ Pharma 11 Twin-screw Extruder (Thermo Fisher, Waltham, MA, USA). The standard screw configuration with four conveying zones and three mixing zones was used in this study, and 100 g batch sizes of PM with the screw rate of 20 RPM was set for the whole extruding process. The extruding temperatures were set between 120 and 170 °C. For the examination, the torque and physical appearance of the filaments were also recorded.

Stability Analysis

The extruded filaments produced by the HME process earlier were milled by mortar and pestle into powder after it was allowed to cool down. The storage stability testing was evaluated under accelerated testing conditions at 40 °C and 75% relative humidity (RH) for a month. XRD was used to evaluate the structural states of the extruded samples.

X-Ray Diffraction (XRD) Analysis

PXRD evaluated the milled extrudates' physical state at zero time point (Tzero) and after 1 month. Analysis was pursued by the D8 ADVANCE ECO diffractometer (Bruker, Billerica, MA, USA). The spectra were collected from the scans within the range of 0.0 to 40.0° at 2-Theta (2θ) with a 0.01° step size and 1 s for per step time.

RESULTS AND DISCUSSIONS

Glass Forming Abilities (GFA)

Applying the DSC method described above, Indo is classified as class 3 by the GFA definition. It suggests that indomethacin is suitable for ASD development since it will not recrystallize easily neither in the first cooling cycle nor the 2nd heating ramp. It will also be beneficial to the ASD formulation's long-term stability. The following studies will further emphasize this result, as discussed below.

Drug-Polymers Miscibility Prediction by Solubility Parameters

Solubility parameters of drugs and polymers were estimated using the Hoftyzer and Van Krevelen method with the information provided in Table I (29). The solubility parameter values obtained for Kollidon® VA 64 was 21.1 MPa$^{1/2}$, and indomethacin solubility parameters were calculated for 23.38 MPa$^{1/2}$. Therefore, the drug-polymer interaction parameter χ calculated by Eq. 13 is 0.5654, slightly above zero. However, since the value is for all compositions ranges, it still suggested that the indomethacin and Kollidon® VA 64 were miscible.

Table I HME Processing Parameters with Physical Appearances

Drug loading (w/w) %	Formulations	Extrusion temperature (°C)	Torque average (%)	Filaments physical appearance
20	F1	120	60 ± 13.0	Opaque with particles
	F2	150	41 ± 8.0	Clear
	F3	160	32.0 ± 6.0	Clear
40	F4	150	51.0 ± 8.0	Clear
	F5	160	37.0 ± 12.0	Clear
	F6	170	30 ± 7.0	Clear

Solubility parameters here were used to suggest drug-polymer miscibility information. It is well-known that compounds with similar solubility parameters (~7 MPa$^{1/2}$) are more likely to be miscible. On the other hand, compounds with solubility parameters differing by more than 10 MPa$^{1/2}$ are more likely to be immiscible (23). In this research, the difference between the solubility parameter of indomethacin and Kollidon® VA 64 was 2.28 MPa$^{1/2}$ which is less than 7 MPa$^{1/2}$. This value suggests that indomethacin is miscible with Kollidon® VA 64. Further thermal analysis should be conducted to examine the possibility of glass-forming ability.

Melting Point Depression

The Indo and Kollidon® VA 64 TGA thermogram showed less than 0.5% weight loss of the pure powder after drying the sample for 2 days, followed by heating to 200 °C. This result verified the drug and polymer's thermal stability and confirmed the MPD method's possibility by DSC heating ramp below.

Usually, the melting point of solid crystalline compounds is the highest when the substance is pure and T_m is depressed in impure solids. In this research, Indo showed melting point depression with the Kollidon® VA 64 as a polymeric carrier across the compositions range, as demonstrated in Fig. 2a. DSC was employed to understand the miscibility between Indo and Kollidon® VA 64 and suggest the optimum drug loading choice for stabilizing the dispersion. Previously, it has been reported that the

solubility of a drug within a polymeric matrix can be determined by measuring melting temperatures (T_m onset from DSC 1st heating ramp) of known different drug-polymer compositions (16, 17). The T_m onset was explored as a reflection of the dissolution of several drug compositions in this research.(18). On the addition of the polymer, MPD occurred relative to the T_m of indomethacin. $(\frac{1}{T_m} - \frac{1}{T_{mo}})$ can be used with Eq. 6 (20). Indo T_m onset decreased with increasing the fraction of Kollidon® VA 64 used, as shown in Fig. 2a. However, this effect is more obvious when drug composition is higher. From Fig. 2b, the endothermic melting peak showed in 1st heating ramp was gone after the rapid cooling, and it only showed one T_g for the system of all drug-polymer compositions (10–90%). Thereby, the DSC heat-cool-heat cycle suggested the formation of Indo-Kollidon® VA 64 ASDs across the drug loading range selected in this study.

Figure 3 shows the predicted and experimental T_g for the drug-polymer binary system. Deviations were observed between experimental T_g and calculated T_g by G-T equation. Positive deviations may show stronger interactions between drug and polymer molecules. On the other hand, negative deviations may reflect weak interactions between drug and polymer molecules. In this study, most compositions selected showed positive deviations of the experimental data from the predicted ones. This result suggested strong interactions between Indo and Kollidon® VA 64 molecules.

A plot of $(1/T_{m\ mix} - 1/T_{m\ pure}) \times (\Delta H_{fus}/-R) - \ln(\varphi_{drug}) - (1 - 1/m)\ \varphi_{polymer}$ *versus* $\varphi_{polymer}^2$, as shown in Fig. 4a,
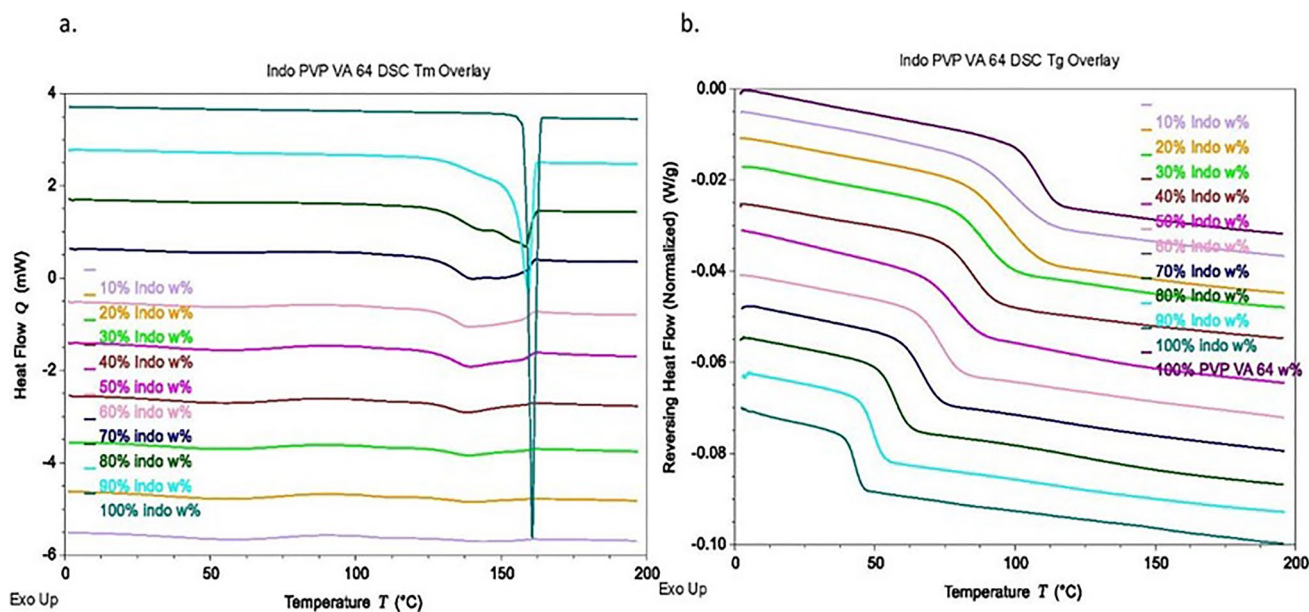

Fig. 2 Indo-Kollidon® VA 64 DSC thermograms overlay. **a** Melting point depression from the 1st heating ramp. **b** ASDs T_g overlay from the 2nd heating ramp
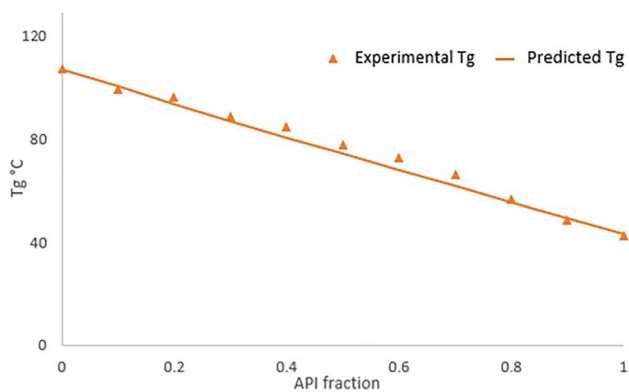
Fig. 3 Indo-Kollidon® VA 64 ASDs T_g of the mixture by DSC (triangle) and G-T equation prediction (solid line)

yielded a linear relationship between these two factors. The Indo-Kollidon® VA 64 system showed a linear relationship across the drug loading range 0.70 to 0.90, and the interaction parameter χ value of -6.7382 ($R^2 = 0.9992$) was obtained. This is characterized by the limited melting point depression data observed from the DSC thermal mixing (Fig. 4). Usually, large positive interaction values were observed for the immiscible drug-polymer binary system through the MPD method. On the other hand, in the current study, the negative χ value suggested Indo and Kollidon® VA 64 were miscible within the compositions range (14). To further understand the drug-polymer miscibility, this study used Eq. 4 and the F–H interaction parameter values (χ) to examine the change in Gibbs free energy as a function of drug volume fraction (Fig. 4b). Gibbs free energy of mixing for this binary system was negative through the composition

range 0.10 to 0.90 at room temperature 25 °C and was dependent upon drug volume fraction and temperature.

Moreover, this study was able to calculate the values for F–H theory A and B constants as manifested in Eq. 7 where A and B values can be used to calculate interaction parameter χ value at different temperatures as shown in Fig. 5 (25, 50, 80, 100, 120, 140, and 160 °C). Therefore, substituting the χ value to Eq. 4 will give us a broader understanding of Gibbs free energy of mixing as a function of drug volume fraction and temperature. This plot helps map the compositions and temperature for spontaneously mixing. It suggested that Kollidon® VA 64 would be miscible with Indo above 100 °C since it showed negative ΔG_{mix}. At 100 °C and
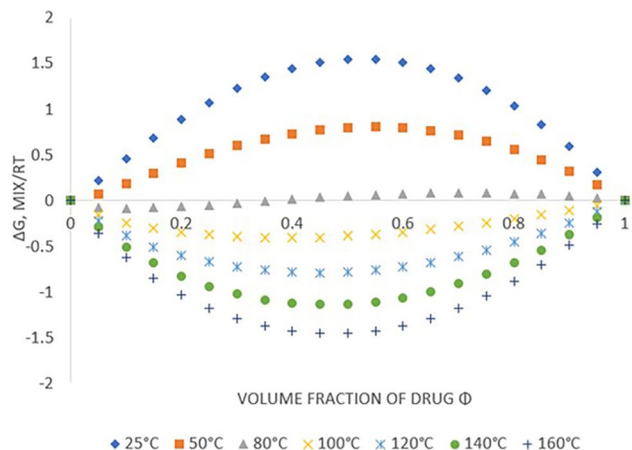

Fig. 5 Gibbs free energy of mixing/RT as a function of Indo volume fraction for model compound and Kollidon® VA 64 system at 25, 50, 80, 100, 120, 140, and 160 °C
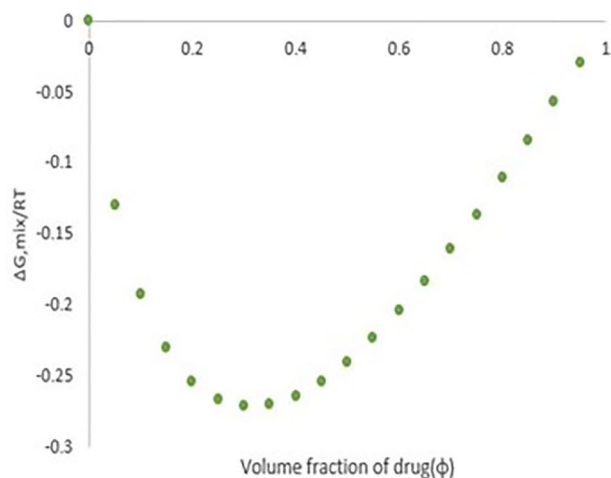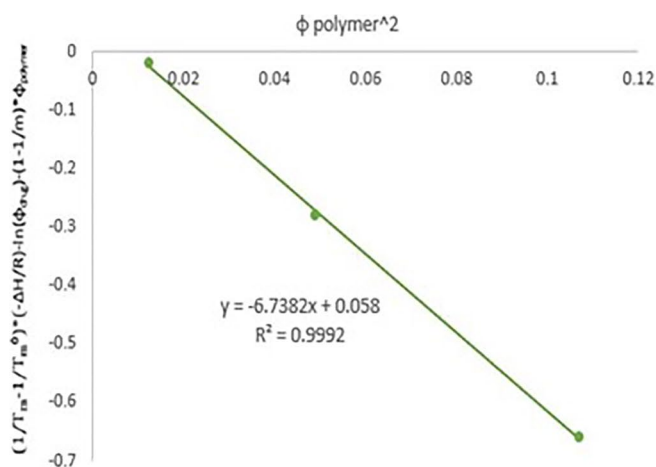

Fig. 4 a F–H interaction parameter plot close to the Indo melting point. **b** Indo-Kollidon® VA 64 system ΔG_{mix}/RT as a function with drug volume fraction

above, Indo-Kollidon® VA 64 binary system will generate a homogenous mixture and are more thermodynamically stable at all drug loading.

Construction of the Phase Diagram

For Indo-Kollidon® VA 64 binary system, this research plotted the ΔG_{mix} as a function of different compositions and temperatures. This information can be combined with T_g to construct the phase diagram, as shown in Fig. 6. The glass transition curve was plotted by the experimental data from DSC 2nd heating cycle. Below the T_g curve, the molecular mobility is low, and the phase separation is thermodynamically favored, so it is usually not considered for ASDs development. Most importantly, this phase diagram identifies the drug-polymer binary system phase boundaries. The drug-polymer solubility curve (liquid–solid boundary) was determined by the melting point depression method. Compounds T_m dropped with the addition of the polymer carrier due to the interaction between drug and polymer. Above the drug-polymer solubility curve (zone A and B), which are considered stable zones, the drug is expected to stay stable in a polymeric carrier, and phase separation is not expected. In general, drugs in this stable range are supersaturated, which can address the drug solubility, dissolution profile, and bioavailability in the gastrointestinal fluids (GI) fluids. Below the drug-polymer solubility curve and above the drug-polymer miscibility curve (zone C and D), which are considered metastable zones. The metastable zone is important to understand the supersaturation and phase separation. In zone C and D, it requires activation energy and kinetics effects to overcome the phase separation. At this

metastable zone, the compound is metastable supersaturated in the polymeric matrix, which helps prevent the precipitation and overall helps to improve the oral dosage absorption. Below the drug-polymer miscibility curve (zones E and F), which are considered unstable zones, phase separation is thermodynamically favored, and it is usually not considered for ASD development.

However, ASD formulation crystallization is a complex process and depends on many thermodynamic factors and storage conditions (*e.g.*, humidity, temperature) and other elements (30). This research constructed a phase diagram with F–H theory by exploring selected drug-polymer compositions' preferences and thermal stability. It is worth knowing that when the system is under room temperature 25 °C, the ASD formulation would very likely be below the system T_g and is perhaps kinetically inhibited from recrystallization, which secures long-term stability. Nevertheless, with the phase diagram, we can determine appropriate compositions and processing conditions that lead to a more stable ASDs system, at least from the thermodynamical consideration.

HME Process Design Space

HME technology is one of the most common ways to produce ASD formulations in the pharmaceutical industry. However, it also has some limitations, especially for thermal-sensitive drugs and polymers. Usually, if the drug T_m is over 200 °C, it has thermal degradation concerns when the processing temperature is set that high during extrusion. Therefore, it is crucial to map the extrusion temperature range to help us avoid thermal degradation and confirm that

Fig. 6 Indo-Kollidon® VA 64 binary system phase diagram
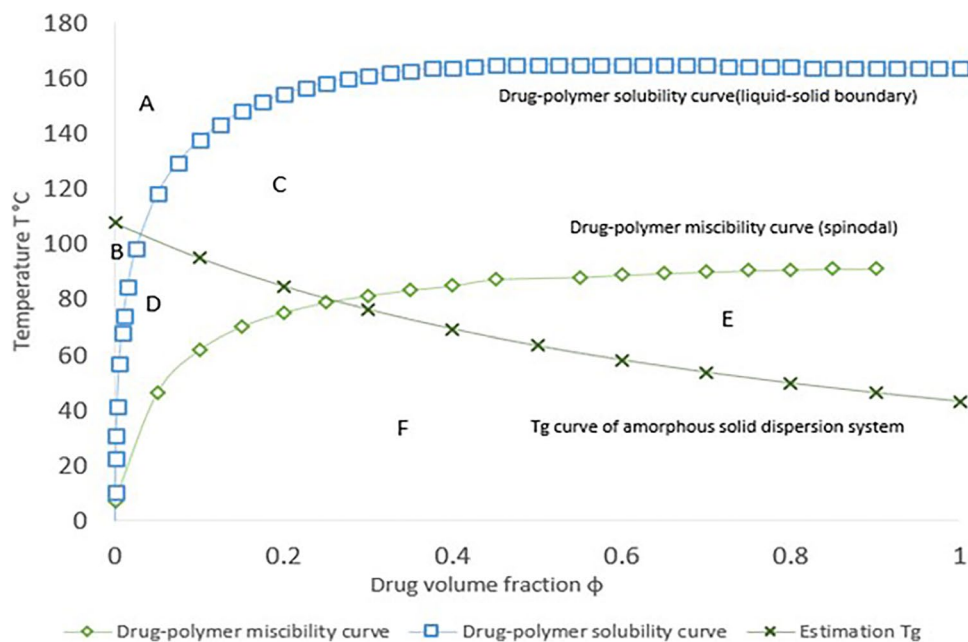
the drug is dispersed in the amorphous form in a polymeric carrier. The phase diagram (Fig. 2a) showed the indomethacin T_m dropped by the addition of the Kollidon® VA 64 under equilibrium conditions, which allow for the production of Indo dispersed ASD at lower processing temperatures even lower than Indo T_m.

Based on the guidance from the phase diagram (Fig. 6), this research identified the stable, metastable, and unstable zone for the Indo-Kollidon® VA 64 system. To extend this study, Fig. 7 clearly illustrated the design space for the HME process, where drug-polymer solubility curve, indomethacin T_m, and the polymer T_{min} dictate (construct) the design space as shown in the green area. The solubility curve obtained from melting point depression helps to select the processing temperature to ensure Indo can fully dissolve in Kollidon® VA 64 polymeric carrier. The crystalline drug compound will convert to its amorphous form in these processing conditions by applying sufficient processing time and conditions. Above the HME process design space, the ASD system may be formed, but it has a higher chance for thermal degradation. Under this design space, the operation most likely will not possess sufficient viscosity and temperature for selected drug loading, so it is expected that the drug could not fully dissolve in the polymeric matrix and will form a suspension.

Preparation of ASDs by HME: Validation of the Phase Diagram

HME processing parameters were selected based on the information suggested by the temperature-composition phase diagram and the HME design space map. This way could reduce the risk of drug degradation. The phase diagram showed that the solubility and miscibility lines both increase as the temperature rises, whereas the T_g curve decreases as the temperature rises. The solubility of Indo

in Kollidon® VA 64 is around 160 °C at 40% drug loading, as per the solubility curve in Fig. 7b. According to the predicted results, the maximum drug loading of Indo at drug melting temperature cannot surpass 40%. To confirm the phase diagram and cover the region until the maximum solubility is reached, 20% and 40% Indo loading were used to stand for the below and maximum drug loading in this case and validate the prediction above. To investigate the temperature impacts on the extruded ASD formulations, formulations of 20% drug loading were extruded at 120 °C, 150 °C, and 160 °C, whereas for 40% drug loading, the extruding temperature was set at 150 °C, 160 °C, and 170 °C. The HME experiments were executed in triplicate. From Figs. 6 to 7b, the maximum solubility of Indo in Kollidon® VA 64 at 20% drug volume fraction is approximately 140 °C. In this case, 120 °C was selected to validate the area under the solubility curve. Most of the processing temperature chose here are under the pure Indo T_m. These process temperatures were selected to represent the stable, metastable, and unstable areas. However, it is difficult to know the physicochemical properties of the filaments based on the phase diagram since the F–H theory did not consider the shearing stress and the mechanical energy input during the extrusion process. Therefore, to obtain further understanding of each formulation (F1-F6), validation was necessary to the different applied temperatures. The average torque and the physical appearance of the filaments are listed in Table I.

Table I showed F1–F6 samples processing parameters and the physical appearance changes of the extruded filaments. The average torque value observed decreased with the increasing extrusion temperature with all formulation batches. For 20% drug loading of indomethacin, it showed the lowest torque at 160 °C processing temperature; and for 40% drug loading of Indo, it showed the lowest torque at 170 °C extruding temperature. Since the other process parameters (screw design, screw speed, die size, die
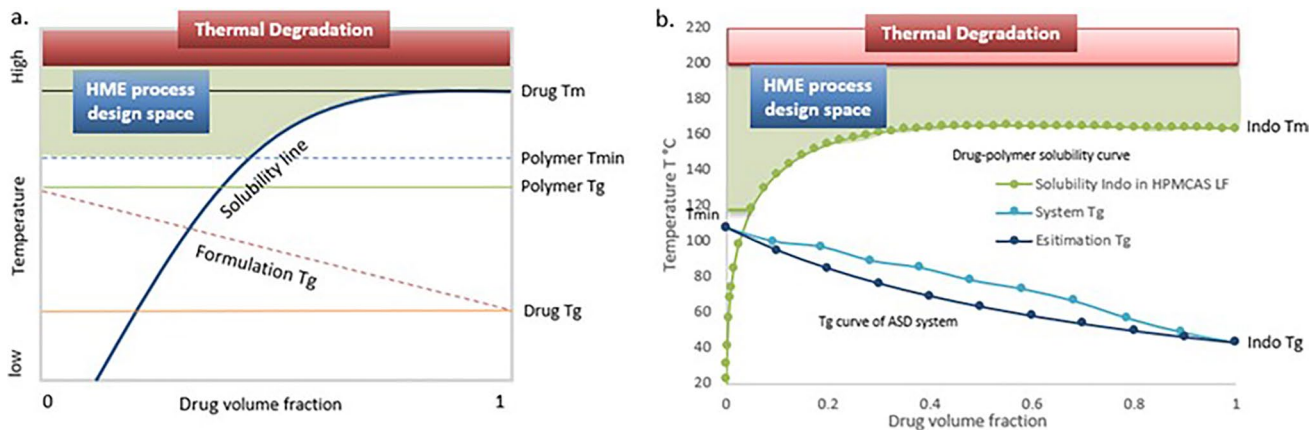

Fig. 7 The temperature-composition phase diagram for HME process design space application
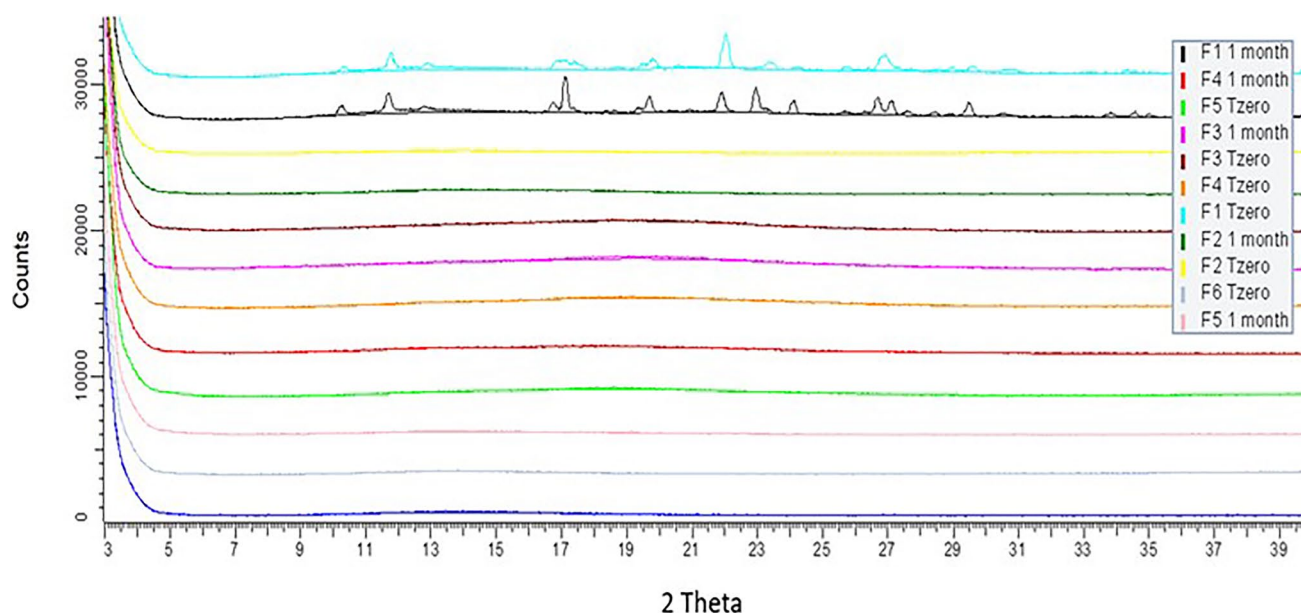
Fig. 8 XRD overlay for ASDs formulation (F1–F6) at Tzero and 1 month under 40 °C/75% RH stability chamber

temperature) were fixed, the impacts of the barrel temperature on the filament's characterization were clearly observed. The filaments at 120 °C were opaque with surface particles. The torque was the highest; this may be explained by insufficient melting of the drug, which led to the drug particle not fully dissolved in the polymer carrier. Other formulation batches showed good physical appearance and can be considered further investigation.

Accelerated Stability Test by PXRD

The filaments obtained from the HME process were milled into powder and stored under accelerated testing conditions at 40 °C and 75% relative humidity (RH) stability chamber for a month. The stability of ASDs formulations was checked using PXRD at the initial development (Tzero) and after exposed in the stability chamber for 1 month. The PXRD results revealed in Fig. 8 confirmed that the amorphization of the Indo in the HME extruded filaments (F2–F6) from Tzero until 1 month under 40 °C/75% RH showed good physical stability of these ASD systems and validated the HME processing setting. F1 formulation (20% Indo) produced under drug-polymer solubility line (120 °C extrusion temperature) showed partial crystallinity at both Tzero and after 1 month. This is likely because the processing temperature was lower than the system T_m, so the drug could not totally transfer to the amorphous state. As shown in Fig. 8, though F4 filaments produced under drug-polymer solubility line (150 °C) showed drug in the amorphous state retained its form after storage, this was likely mediated by strong drug-polymer molecular interactions in addition to

the processing temperature (150 °C) close to the binary curve at 40% drug loading. On the other hand, it confirmed that the phase diagram and the HME processing are necessary for optimizing the producing parameters.

CONCLUSION

This research has proposed a lab-scale method based on the F–H theory to predict the solubility and miscibility of the drug-polymer binary system. Indo and Kollidon® VA 64 interaction parameters were obtained by melting point depression and solubility parameter methods. The temperature-composition and Gibbs free energy of mixing phase diagrams above the system T_g were constructed. The phase diagram clarifies the stable, metastable, and unstable zone for the ASDs system. The phase diagram provides a reasonable design space for the HME process of ASDs with the kinetic and thermodynamic considerations allowing for extrusion process at lower temperatures besides inhibiting the recrystallization. This work established fundamental thermodynamic elements for the HME process design as well as the process development.

Abbreviations ASD: Amorphous solid dispersion; HME: Hot melt extrusion; Indo: Indomethacin; PVP VA 64: Polyvinyl pyrrolidone vinyl acetate; Kollidon® VA 64: Polyvinyl pyrrolidone vinyl acetate; F–H theory: Flory-Huggins theory; G-T equation: Gordon-Taylor equation; BCS: Biopharmaceutical classification system; DSC: Differential scanning calorimetry; TGA: Thermogravimetric analysis; Eq: Equation; χ: Interaction parameter; T_g: Glass transition temperature; $T_{g\mathrm{mix}}$: ASDs glass transition temperature; T_{g1}: Drug glass

transition temperature; T_{g2}: Polymer glass transition temperature; w_1: Drug weight fraction; w_2: Polymer weight fraction; φ: Drug volume fraction; $\varphi_{polymer}$: Polymer volume fraction; $1-\varphi$: Polymer volume fraction; ρ_1: Drug density; ρ_2: Polymer density; K: Adjustable fitting parameter; T_m: Melting point temperature; ΔG_{mix}: Gibbs free energy of mixing; ΔH_{mix}: The change in enthalpy; ΔS_{mix}: The change in entropy; δ_t: Solubility parameter; δ_d: Components of disperse forces; δ_p: Components of polar group forces; δ_h: Components of hydrogen bond energy; F_{di}: Group contribution to the disperse forces,; E_{hi}: Group contribution to hydrogen bonding energy; F_{pi}: Plane symmetry factor of polar groups; V_0: Group contributions to the molar volume; R^2: R-Squared; GFA: Glass forming abilities; MPD: Melting point depression; UCST: Upper critical solution temperature; T_{min}: Minimum processing temperature; GI fluids: Gastrointestinal fluids; PM: Physical mixture; T_{deg}: Degradation temperature; XRD: X-ray diffraction; PXRD: Powder X-ray diffraction; θ: Theta; *RH*: Relative humidity

Declarations

References

1. Leuner C, Dressman J. Improving drug solubility for oral delivery using solid dispersions. Eur J Pharm Biopharm. 2000;50(1):47–60. https://doi.org/10.1016/s0939-6411(00)00076-x.

2. Repka MA, Bandari S, Kallakunta VR, Vo AQ, McFall H, Pimparade MB, Bhagurkar AM. Melt extrusion with poorly soluble drugs–an integrated review. Int J Pharm. 2018;535(1–2):68–85. https://doi.org/10.1016/j.ijpharm.2017.10.056.

3. Yu L. Amorphous pharmaceutical solids: preparation, characterization and stabilization. Adv Drug Deliv Rev. 2001;48(1):27–42. https://doi.org/10.1016/s0169-409x(01)00098-9.

4. Vasconcelos T, Sarmento B, Costa P. Solid dispersions as strategy to improve oral bioavailability of poor water soluble drugs. Drug Discovery Today. 2007;12(23–24):1068–75. https://doi.org/10.1016/j.drudis.2007.09.005.

5. Hancock BC, Parks M. What is the true solubility advantage for amorphous pharmaceuticals? Pharm Res. 2000;17(4):397–404. https://doi.org/10.1023/a:1007516718048.

6. Brouwers J, Brewster ME, Augustijns P. Supersaturating drug delivery systems: the answer to solubility-limited oral bioavailability? J Pharm Sci. 2009;98(8):2549–72. https://doi.org/10.1002/jps.21650.

7. Abu-Diak OA, Jones DS, Andrews GP. An investigation into the dissolution properties of celecoxib melt extrudates: understanding the role of polymer type and concentration in stabilizing supersaturated drug concentrations. Mol Pharm. 2011;8(4):1362–71. https://doi.org/10.1021/mp200157b.

8. Serajuddin AT. Solid dispersion of poorly water - soluble drugs: early promises, subsequent problems, and recent breakthroughs. J Pharm Sci. 1999;88(10):1058–66. https://doi.org/10.1021/js980403l.

9. Shanbhag A, Rabel S, Nauka E, Casadevall G, Shivanand P, Eichenbaum G, Mansky P. Method for screening of solid dispersion formulations of low-solubility compounds—miniaturization and automation of solvent casting and dissolution testing. Int J Pharm. 2008;351(1–2):209–18. https://doi.org/10.1016/j.ijpharm.2007.09.042.

10. Zheng W, Jain A, Papoutsakis D, Dannenfelser RM, Panicucci R, Garad S. Selection of oral bioavailability enhancing formulations during drug discovery. Drug Dev Ind Pharm. 2012;38(2):235–47. https://doi.org/10.3109/03639045.2011.602406.

11. Marsac PJ, Shamblin SL, Taylor LS. Theoretical and practical approaches for prediction of drug–polymer miscibility and solubility. Pharm Res. 2006;23(10):2417–26. https://doi.org/10.1007/s11095-006-9063-9.

12. Abu-Diak OA, Jones DS, Andrews GP. Understanding the performance of melt-extruded poly (ethylene oxide)–bicalutamide solid dispersions: characterisation of microstructural properties using thermal, spectroscopic and drug release methods. J Pharm Sci. 2012;101(1):200–13. https://doi.org/10.1002/jps.22748.

13. Gupta J, Nunes C, Vyas S, Jonnalagadda S. Prediction of solubility parameters and miscibility of pharmaceutical compounds by molecular dynamics simulations. J Phys Chem B. 2011;115(9):2014–23. https://doi.org/10.1021/jp108540n.

14. Marsac PJ, Li T, Taylor LS. Estimation of drug–polymer miscibility and solubility in amorphous solid dispersions using experimentally determined interaction parameters. Pharm Res. 2009;26(1):139–51. https://doi.org/10.1007/s11095-008-9721-1.

15. Paudel A, Van Humbeeck J, Van den Mooter G. Theoretical and experimental investigation on the solid solubility and miscibility of naproxen in poly (vinylpyrrolidone). Mol Pharm. 2010;7(4):1133–48. https://doi.org/10.1021/mp100013p.

16. Tao J, Sun Y, Zhang GG, Yu L. Solubility of small-molecule crystals in polymers: D-mannitol in PVP, indomethacin in PVP/VA, and nifedipine in PVP/VA. Pharm Res. 2009;26(4):855–64. https://doi.org/10.1007/s11095-008-9784-z.

17. Sun YE, Tao J, Zhang GG, Yu L. Solubilities of crystalline drugs in polymers: an improved analytical method and comparison of solubilities of indomethacin and nifedipine in PVP, PVP/VA, and PVAc. J Pharm Sci. 2010;99(9):4023–31. https://doi.org/10.1002/jps.22251.

18. Caron V, Tajber L, Corrigan OI, Healy AM. A comparison of spray drying and milling in the production of amorphous dispersions of sulfathiazole/polyvinylpyrrolidone and sulfadimidine/polyvinylpyrrolidone. Mol Pharm. 2011;8(2):532–42. https://doi.org/10.1021/mp1003674.

19. Rubinstein M. Polymer physics—The ugly duckling story: will polymer physics ever become a part of "proper" physics? J Polym Sci, Part B: Polym Phys. 2010;48(24):2548–51. https://doi.org/10.1002/polb.22135.

20. Lin D, Huang Y. A thermal analysis method to predict the complete phase diagram of drug–polymer solid dispersions. Int J Pharm. 2010;399(1–2):109–15. https://doi.org/10.1016/j.ijpharm.2010.08.013.

21. Hoei Y, Yamaura K, Matsuzawa S. A lattice treatment of crystalline solvent-amorphous polymer mixtures on melting point depression. J Phys Chem. 1992;96(26):10584–6. https://doi.org/10.1021/j100205a002.

22. Silva MA, De Paoli MA, Felisberti MI. Flory-Huggins interaction parameter of poly (ethylene oxide)/poly (epichlorohydrin) and poly (ethylene oxide)/poly (epichlorohydrin-co-ethylene oxide) blends. Polymer. 1998;39(12):2551–6. https://doi.org/10.1016/S0032-3861(97)00574-0.

23. Baird JA, Van Eerdenbrugh B, Taylor LS. A classification system to assess the crystallization tendency of organic molecules from undercooled melts. J Pharm Sci. 2010;99(9):3787–806. https://doi.org/10.1002/jps.22197.

24. Blaabjerg LI, Lindenberg E, Löbmann K, Grohganz H, Rades T. Glass forming ability of amorphous drugs investigated by continuous cooling and isothermal transformation. Mol Pharm. 2016;13(9):3318–25. https://doi.org/10.1021/acs.molpharmaceut.6b00650.

25. Barton AF. CRC handbook of solubility parameters and other cohesion parameters. Routledge; 2017.

26. Bhugra C, Pikal MJ. Role of thermodynamic, molecular, and kinetic factors in crystallization from the amorphous state. J Pharm Sci. 2008;97(4):1329–49. https://doi.org/10.1002/jps.21138.

27. Li S, Tian Y, Jones DS, Andrews GP. Optimising drug solubilisation in amorphous polymer dispersions: rational selection of hot-melt extrusion processing parameters. AAPS PharmSciTech. 2016;17(1):200–13. https://doi.org/10.1208/s12249-015-0450-6.

28. Newman A, Knipp G, Zografi G. Assessing the performance of amorphous solid dispersions. J Pharm Sci. 2012;101(4):1355–77. https://doi.org/10.1002/jps.23031.

29. Moseson DE, Taylor LS. The application of temperature-composition phase diagrams for hot melt extrusion processing of amorphous solid dispersions to prevent residual crystallinity. Int J Pharm. 2018;553(1–2):454–66. https://doi.org/10.1016/j.ijpharm.2018.10.055.

30. Forster A, Hempenstall J, Tucker I, Rades T. Selection of excipients for melt extrusion with two poorly water-soluble drugs by solubility parameter calculation and thermal analysis. Int J Pharm. 2001;226(1–2):147–61. https://doi.org/10.1016/S0378-5173(01)00801-8.

31. Just S, Sievert F, Thommes M, Breitkreutz J. Improved group contribution parameter set for the application of solubility parameters to melt extrusion. Eur J Pharm Biopharm. 2013;85(3):1191–9. https://doi.org/10.1016/j.ejpb.2013.04.006.

Publisher's note Springer Nature remains neutral with regard to jurisdictional claims in published maps and institutional affiliations.